MOLECULAR AND CELLULAR BIOLOGY, Feb. 2009, p. 1035–1049 Vol. 29, No. 4
0270-7306/09/$08.00+0 doi:10.1128/MCB.00336-08

The Transforming Rho Family GTPase Wrch-1 Disrupts Epithelial Cell Tight Junctions and Epithelial Morphogenesis▽

Donita C. Brady,[1] Jamie K. Alan,[1] James P. Madigan,[2] Alan S. Fanning,[3] and Adrienne D. Cox[1,2,4,5]*

Department of Pharmacology,[1] Curriculum in Genetics and Molecular Biology,[2] Department of Cell and Molecular Physiology,[3] Department of Radiation Oncology,[4] and Lineberger Comprehensive Cancer Center,[5] University of North Carolina at Chapel Hill, Chapel Hill, North Carolina 27599

Received 27 February 2008/Returned for modification 17 March 2008/Accepted 20 November 2008

Wrch-1, an atypical and transforming Rho GTPase, regulates cellular activities including proliferation and actin organization, but its functions and effectors remain poorly characterized. We show here that Wrch-1 distributes along the apical and basolateral membranes in MDCK cells and binds the cell polarity protein Par6 in a GTP-dependent manner. Activated Wrch-1 negatively regulates the kinetics of tight junction (TJ) assembly during epithelial cell polarization but has no detectable effect on overall cell polarity in confluent monolayers. It also causes a dramatic cytoskeletal reorganization and multilayering in cells grown in two-dimensional culture and disrupts cystogenesis of cells grown in three-dimensional (3D) culture. Similarly, short hairpin RNA-mediated knockdown of Wrch-1 perturbs cystogenesis in 3D culture, suggesting that tight regulation of Wrch-1 activity is necessary for normal epithelial morphogenesis. A weakly transforming effector domain mutant of activated Wrch-1 that inhibits Par6 binding abrogates the ability of Wrch-1 to disrupt TJ formation, actin organization, and epithelial morphogenesis. We hypothesize that Wrch-1-induced morphological and growth transformation may occur in part through Par6-mediated disruption of TJs and actin organization.

Rho family small GTPases are Ras-related proteins that regulate many normal cellular properties such as cell shape, cell motility and migration, gene transcription, and cell proliferation (10). Like other members of the Ras superfamily, Rho GTPases function as molecular switches cycling between an active GTP-bound state and inactive GDP-bound state (44). When GTP bound and active, they elicit biological functions through interactions with their downstream effectors (16).

Wrch-1 is an atypical member of the Cdc42 subgroup of Rho GTPases that are perhaps best known for inducing the formation of actin microspikes and filopodia. Wrch-1 shares 57% sequence identity with Cdc42 and 61% sequence identity with its close relative, Chp/Wrch-2 (3, 45). Despite this high sequence identity, Wrch-1 has unique characteristics that suggest regulation and biological functions divergent from those of each of these relatives. For example, Wrch-1 was initially discovered as a Wnt1-responsive gene that, when mutationally activated (Q107L, analogous to the Q61L mutation in Ras and Cdc42), phenocopied Wnt-1 morphological transformation (45). Recent studies have highlighted an additional role for Wrch-1 in the regulation of cell migration through mechanisms clearly distinct from those of Cdc42, such as modulating focal adhesion turnover (8, 30). In addition, Wrch-1 contains a 46-amino-acid N-terminal extension not found in Cdc42. This extension contains poly-proline PxxP binding motifs that facilitate interactions with Src homology 3 (SH3) domain-containing proteins such as Grb2, phospholipase Cγ, and NCKβ (39, 42). We and others have shown that expression of activated Wrch-1 leads to activation of PAK1 and Jun N-terminal protein kinase (JNK), formation of filopodia, and cellular transformation of NIH 3T3 fibroblasts (5, 39). Although some of the biochemical characteristics, subcellular localization, and membrane association properties of Wrch-1 have been identified, full identification and characterization of Wrch-1 downstream effectors, regulators, biological functions, and potential contributions to cancer remain elusive.

A yeast two-hybrid screen using Wrch-1 as the bait identified two proteins as potential interacting partners: Par6 and PAK1b (4). Par6 is known to form an evolutionarily conserved complex with protein kinase C ζ (PKC ζ) and Par3 that is instrumental in establishing epithelial cell polarity and in regulating tight junction (TJ) formation (14, 41). This suggested the possibility that Wrch-1 might have similar functions and thus share a critical role in many aspects of normal cell and tissue homeostasis. Classic Rho GTPases, including Rac1 and Cdc42, are known to participate in the formation of TJs through interactions with the cell polarity proteins Par6 and Par3. Aberrant activation of these GTPases is known to disrupt TJs and cell polarity and to induce epithelial cell transformation (7, 17, 18, 33, 36). Whether Wrch-1 or other atypical Cdc42-related proteins also participate in TJ regulation or cause transformation of epithelial cells remains to be tested.

The ability of Rho GTPases to regulate actin cytoskeletal dynamics is another factor that regulates TJ dynamics and integrity (6, 27). In epithelial cells, the actin cytoskeleton is enriched at the apical surface and forms a contractile ring anchored to adherens junctions (AJs) and TJs which is required to maintain proper epithelial cell shape and function. Actomyosin-based contraction of both this actin ring and an array of basal stress fibers occurs during processes such as cell polarization and epithelial morphogenesis. Anchoring of the actin cytoskeleton to cell junctions integrates cell-cell contacts

* Corresponding author. Mailing address: Departments of Radiation Oncology and Pharmacology, 1028 NCCCC, 101 Manning Drive, CB # 7512, University of North Carolina at Chapel Hill, Chapel Hill, NC 27599-7512. Phone: (919) 966-7713, ext. 305. Fax: (919) 966-7681. E-mail: adrienne_cox@med.unc.edu.

▽ Published ahead of print on 8 December 2008.

with changes in cell morphology and with morphogenetic movements of epithelial cells that occur during organogenesis (21). Whether Wrch-1 regulation of the actin cytoskeleton is a potential mechanism for modulating epithelial cell morphology remains to be determined.

One of the earliest steps of tumor initiation and progression in epithelial cells is the loss of their polarized morphology, which is a process that involves the loss of cell-cell adhesions, loss of cell polarization, and reorganization of the cytoskeleton. Together, these changes promote dedifferentiation and are also required for later invasion and metastasis (38). Misregulation of Rho GTPases has been shown to lead to aberrant growth, dedifferentiation, invasion, and metastasis (9). Wrch-1 message is differentially expressed in a variety of human tumors (20), suggesting that its aberrant function may also contribute to oncogenesis. Whether Wrch-1 expression or activation contributes to tumorigenesis or other disease pathologies is unknown.

In the present study, we sought to determine whether Wrch-1 regulates epithelial cell morphology through modulating TJs, cell polarity, and the actin cytoskeleton and whether the loss of normal cell morphology contributes to Wrch-1-mediated transformation. Specifically, we investigated a potential interaction between Wrch-1 and the cell polarity protein Par6 and we used polarized epithelial cells to elucidate whether expression of Wrch-1 affects epithelial cell TJ assembly and actin organization. We also investigated whether any such effects are connected with anchorage-independent growth, a hallmark of transformation, and with loss of three-dimensional (3D) morphogenesis, a hallmark of dedifferentiation that is necessary for invasion and metastasis. We demonstrate that Wrch-1 expression is required for epithelial morphogenesis and that activated Wrch-1 has dramatic effects on cytoskeletal organization, epithelial morphogenesis, and TJ assembly. These observations reveal a potential mechanism by which Wrch-1 may control normal cell morphology and contribute to Wrch-1-mediated transformation of epithelial cells.

MATERIALS AND METHODS

Cell culture, transfection, and retroviral infection. COS-7 cells were grown in Dulbecco's modified Eagle's medium (GIBCO/Invitrogen) supplemented with 10% fetal bovine serum (Sigma) and 1% penicillin-streptomycin and maintained in 5% CO_2 at 37°C. Cells were transfected using TransIT-LT1 (Mirus) according to the manufacturer's instructions.

MDCKII cells, generously provided by Robert Nicholas (University of North Carolina—Chapel Hill [UNC-CH]), were grown as described above and supplemented with 1% nonessential amino acids (Invitrogen) ("complete medium"). Stable MDCKII cell lines were generated by retroviral infection. Production of retrovirus was obtained by $CaCl_2$-mediated transfection of pBabe-HAII-puro, pVPack-Gag/Pol, and pVPack-Ampho (Stratagene) vectors into 293T cells. Cells were infected by exposure to retroviral supernatant containing 8 μg/ml of Polybrene (American Bioanalytical) and maintained in puromycin for 10 days, after which colonies were pooled for use. MDCKII cell lines stably expressing HuSH pRS short hairpin RNA (shRNA) (OriGene) vectors were generated by retroviral infection as described above. Cystogenic growth in 3D collagen I gels was performed as described previously (28, 29).

Molecular constructs. Human Wrch-1 proteins (wild type [WT] or Q107L, ΔN-WT, ΔN-Q107L, and Q107L C255S C256S) were generated as described previously (5). For hemagglutinin (HA) epitope-tagged Wrch-1, 5′ and 3′ BamHI sites were introduced by PCR for ligation into the BamHI site of pCGN-hygro or pBabe-HAII-puro retroviral expression vectors. Human Wrch-1(Q107L F86C) was generated by site-directed mutagenesis and subcloned as described above. To generate Myc- and glutathione *S*-transferase (GST)-tagged human Par6, PCR was used to introduce 5′ BamHI and 3′ EcoRI sites into a pBabe-T7-Par6C construct (gift of Channing Der, UNC-CH) for subcloning into pCMV3B(Myc) and pGEX4T(GST), respectively. Wrch-1-specific and negative control noneffective green fluorescent protein (GFP)-directed shRNA expression vectors were purchased from OriGene. The pRS-shWrch-1 no. 1 plasmid contains a 29-bp shRNA cassette directed against the Wrch-1 target sequence 5′ CAGAGAAGATGTCAAAGTCCTCATTGAG 3′, whereas the pRS-shWrch-1 no. 2 plasmid contains a 29-bp shRNA cassette directed against Wrch-1 target sequence 5′ CCGTGAGACTCCAACTCTGTGACACTGCC 3′. All sequences were verified by the Genome Analysis Facility at UNC-CH.

Western blot analysis. Cells were lysed in magnesium lysis buffer (MLB) (25 mM HEPES [pH 7.5], 150 mM NaCl, 1% NP-40, 0.25% Na deoxycholate, 10% glycerol, 10 mM $MgCl_2$, and complete protease inhibitor tablet [Roche]) or 1% Triton X-100 containing 1× protease inhibitor cocktail (Roche). Cell lysates were cleared by centrifugation, and protein concentrations were determined using the D. C. Lowry protein assay (Bio-Rad). Samples were prepared in 5× sample buffer, and 20 μg of protein for each sample was resolved by 12% or 8% sodium dodecyl sulfate-polyacrylamide gel electrophoresis (SDS-PAGE). Proteins were transferred to polyvinylidene difluoride (Millipore), blocked overnight in 3% fish gelatin (Sigma), and incubated with anti-HA (HA.11; Covance), anti-Myc (9E10; Covance), anti-GST (Covance), and anti-β-actin (Sigma). Washed membranes were incubated in anti-mouse or anti-rabbit immunoglobulin G-horseradish peroxidase (Amersham Biosciences) or anti-mouse kappa light chain-horseradish peroxidase (Zymed), washed again, and developed using SuperSignal West Dura extended-duration substrate (Pierce).

Reverse transcription-PCR. For reverse transcription-PCR, total RNA was isolated from MDCK cells using the RNeasy kit (Qiagen). To generate cDNA, RNA was primed with oligo(dT) primer and reverse transcription was catalyzed using Superscript III reverse transcriptase (Invitrogen). PCR was performed using *Taq* DNA polymerase (Invitrogen) and primers for Wrch-1 (5′ CGAG TACTGAATGCCAGCAA and 3′ TGAGCTGGACAAATGCAAAG) and actin (5′ GCTCGTCGTCGACAACGGCTC and 3′ CAAACATGATCTGGGT CATCTT). The resulting product was resolved on a 2% agarose gel and visualized under UV light. Each experiment was run in triplicate, and densitometry was performed using Image-J software.

GST-pulldown assays and immunoprecipitation. COS-7 cells were lysed 24 h after transfection in MLB, and the lysates were precleared with GST-Sepharose beads. Precleared lysates were incubated with GST or GST-Par6C beads. GST-Par6 was purified as described previously (13). Beads were collected and washed with MLB and resuspended in sample buffer. SDS-PAGE analysis and immunoblotting were performed as described above.

COS-7 cells were lysed 48 h after transfection in MLB. Precleared lysates were incubated with mouse anti-Myc antibody, and the immunoprecipitates were collected with protein G Plus-Sepharose beads (Zymed). SDS-PAGE analysis and immunoblot were performed as described above.

Calcium switch. MDCKII cells were plated on 12-mm Transwell filters (Corning-Costar) for 4 h in normal calcium medium (NCM; 1.8 mM Ca^{2+}). After attachment, cells were rinsed gently with suspension minimum essential medium (Gibco/Invitrogen) and then incubated in low calcium medium (LCM; 5 μM Ca^{2+}) overnight to disrupt cell-cell contacts. After 18 h, calcium was restored (calcium switch) by replacement of LCM with NCM.

TER and paracellular permeability assays. To measure transepithelial resistance (TER), MDCKII cells were plated on 12-mm Transwell filters at 5.0×10^5 cells per cm^2 of filter and subjected to calcium switch. TER ($\Omega \times cm^2$) was measured using an epithelial volt-ohmmeter (World Precision Instruments). Three separate filters were used for each cell line, and the mean resistance was calculated after subtraction of the background resistance from a filter containing only culture medium.

Paracellular flux was measured in MDCKII cells subjected to calcium switch. After incubation in LCM, NCM containing 2 mg/ml of 4,000-kDa fluorescein isothiocyanate (FITC)-dextran or 40,000-kDa FITC-dextran tracer (Sigma) was placed in the apical chamber and NCM without tracer was placed in the basal chamber. Monolayers were incubated in NCM for 6 h at 37°C, and the basal chamber media was collected. FITC-dextran tracer was measured with a microplate spectrofluorometer (excitation of 492 nm and emission of 520 nm; SpectraMax Gemini).

IF analysis. Immunofluorescence (IF) analysis of protein expression and localization in cells grown on filters was performed as described previously (48). Briefly, fixed and permeabilized MDCKII cells were incubated overnight in antibodies to HA (mouse; Covance), zonula occludens 1 (ZO-1; rabbit [Zymed]), β-catenin (rabbit; Sigma), E-cadherin (rat; Sigma), occludin (rabbit); and/or Par3 (rabbit; Upstate). Cells were then washed and incubated overnight in secondary antimouse, antirabbit, or antirat antibodies conjugated to Alexa 488, Alexa 594, or Alexa 647, respectively, and/or with Texas Red-phalloidin (Mo-

lecular Probes). After antibody treatment, filters were mounted on glass slides for imaging.

Staining of MDCKII cysts grown in 3D collagen was performed as described previously (29, 35). Briefly, collagen gels containing MDCKII cells were treated with collagenase type VII (Sigma C-2399), fixed and permeabilized, and then incubated in antibodies and mounted for imaging as described above.

Confocal microscopy was performed on an Olympus Fluoview 300 laser-scanning confocal imaging system configured with an IX70 fluorescence microscope fitted with a PlanApo ×60 oil objective. Images were acquired with the use of Olympus Fluoview software and subsequently resized in Adobe Photoshop. Multiple *xy* and *xz* scans were acquired for each monolayer of cells or 3D collagen gel.

Growth transformation assay. Single-cell suspensions of MDCKII cells (3.5×10^3 cells per 35-mm dish) were suspended in 0.4% agar (BD Biosciences) in complete medium and layered on top of 0.6% agar as described previously (42). After 14 days, colonies were stained with 3-(4,5-dimethylthiazol-2-yl)-2,5-diphenyltetrazolium bromide (MTT; Sigma), and the average number of colonies on triplicate dishes was calculated.

RESULTS

Wrch-1 interacts with the cell polarity protein Par6 in a GTP-dependent manner. The function of Rho GTPases is dictated by their subcellular localization and interaction with downstream effectors. Therefore, the observation that active GTP-bound Wrch-1 interacts with the cell polarity protein Par6 in a yeast two-hybrid screen (4) suggested a possible role for Wrch-1 in regulating cell polarity. To determine whether GTP–Wrch-1 and Par6 interact in vitro and whether the interaction is nucleotide dependent, we expressed Par6 as a GST fusion protein in *E. coli* and performed GST-Par6 pulldowns from lysates of COS-7 cells expressing Wrch-1 proteins. As predicted by the yeast two-hybrid screen, we found that both WT and constitutively activated Wrch-1(Q107L) interacted with GST-Par6 (Fig. 1A) but not with GST-alone controls (data not shown), whereas GDP-bound Wrch-1(T63N) did not interact. We also observed that N-terminally truncated ΔN-Wrch-1(Q107L) still bound to Par6 (Fig. 1A), indicating that this interaction does not require the polyproline-rich N-terminal extension. To further investigate this interaction, we coexpressed the HA-tagged Wrch proteins with Myc-tagged Par6 in COS-7 cells and assessed their interaction by immunoprecipitation. As predicted by our in vitro GST pulldowns, GTP-bound WT Wrch-1 or Wrch-1(Q107L) but not GDP-bound Wrch-1(T63N) associated with imunoprecipitated Par-6 (Fig. 1B). These data show that the cell polarity protein, Par6, associates with Wrch-1 both in vitro and in vivo in a GTP-dependent manner, supporting the notion that it could be a physiological effector of Wrch-1 function.

Wrch-1 localizes to cell-cell junctions in polarized MDCKII cells. The Par6-PKC ζ complex regulates the formation of epithelial cell junctions that are required for normal epithelial cell polarity and morphology (49), and the interaction of Wrch-1 with this complex suggested that Wrch-1, like Par6 and PKC ζ, may also localize at these junctions in polarized cells. Therefore we used confocal microscopy to visualize Wrch-1 localization in polarized MDCKII epithelial cells stably expressing HA-tagged Wrch-1 proteins. Wrch-1 localized to the plasma membrane (PM) and to microvilli at the apical surface, but was associated predominantly with the basolateral PM (Fig. 2A). Unfortunately, we were unable to characterize the distribution of endogenous Wrch-1 in MDCKII because there is no existing antibody capable of detecting endogenous Wrch-1.

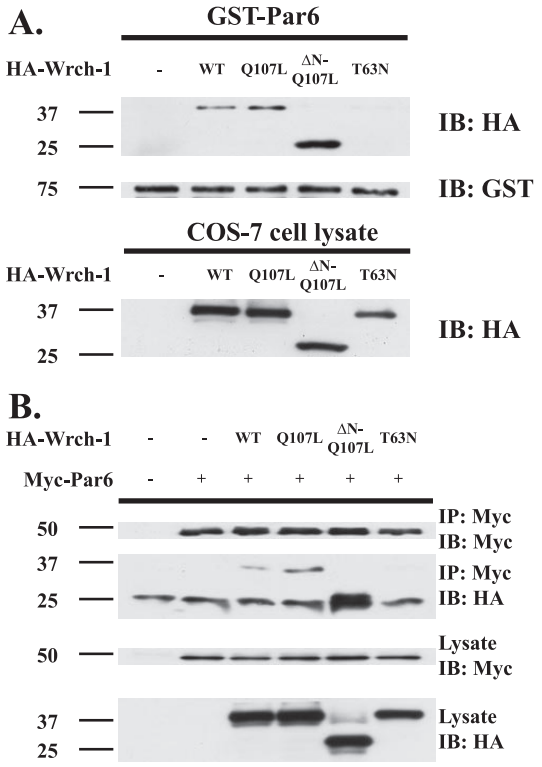

FIG. 1. GTP-bound Wrch-1 interacts with Par6 in vitro and in vivo. (A) COS-7 cell lysates expressing empty vector or HA-tagged Wrch-1 constructs were incubated with GST alone or GST-Par6, and the presence of Wrch-1 in the pulldown was probed by Western blot (immunoblot [IB]) analysis with anti-HA antibody. Pulldown of GST-Par6 was confirmed with anti-GST antibody. (B) COS-7 cells were cotransfected with empty vector or HA-tagged Wrch-1 along with Myc-tagged Par6. Par6 was immunoprecipitated (IP) with anti-Myc antibody, and immunoprecipitates were probed for Wrch-1 by immunoblotting with anti-HA antibody.

We then attempted to determine whether Wrch-1 colocalizes with components of the polarity complex. Due to the lack of commercially available antibodies that can effectively detect Par6 by IF, we used antibodies against Par3, which is known to associate with both Par6 and PKC ζ at TJ in polarized MDCKII cells (15). In empty vector control MDCKII cells, Par3 was restricted to a defined band at cell-cell contact regions known as the apical junctional complex (AJC) (Fig. 2B, *xz* scans). As described above, WT Wrch-1 was distributed all along the lateral cell contacts but clearly overlapped with endogenous Par3 at the AJC (Fig. 2B). This partial overlap is not unexpected, because we anticipate that Wrch-1 has multiple functions in epithelial cells, not all of which are linked to its interaction with Par6.

The distribution of Wrch-1 predominantly to basolateral membranes is consistent with its potential association with cell-cell junctions, such as TJs and AJs. TJs are the most apical of cell junctions, and TJ proteins such as occludin and ZO-1, like Par6, are generally restricted to a tight band that circumscribes the AJC. AJs are adhesive structures formed through calcium-dependent interactions between cadherin molecules on adjacent epithelial cells, and AJ proteins such as E-cadherin and β-catenin localize to both the AJC and along the entire

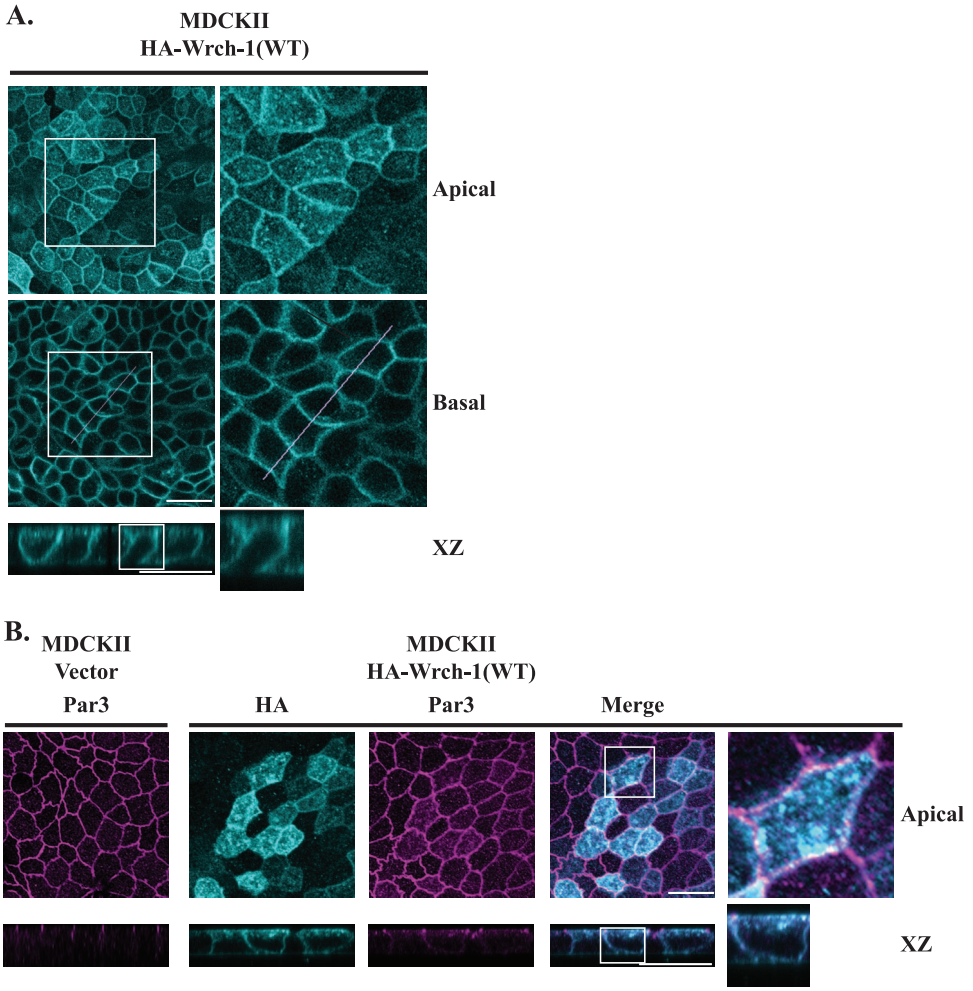

FIG. 2. Wrch-1 displays overlapping localization with the cell polarity protein Par3 in polarized MDCKII cells. Cells stably expressing empty vector or HA-tagged Wrch-1 were grown to confluence on 12-mm Transwell filters and then fixed and stained using primary antibodies against the HA epitope tag alone (cyan) (A) or either the HA epitope tag (cyan) or Par3 (magenta) (B). IF staining was visualized using a confocal microscope. Square panels, *xy* sections; rectangular panels, *xz* sections (top to bottom). Scale bars, 20 μm.

lateral PM. To investigate the possibility that Wrch-1 localizes to both TJs and AJs in polarized epithelial cells, we examined MDCKII cells stably expressing WT HA–Wrch-1. Wrch-1 localized at the lateral PM overlapped with the TJ transmembrane protein, occludin, and with the TJ peripheral protein, ZO-1, but did not localize exclusively to TJs (Fig. 3A and B, top panels). The partial overlap between these proteins at cell-cell contact regions (Fig. 3A and B, *xz* scans) suggests that the spatial distribution of Wrch-1 may allow it to regulate TJs.

We also used IF to investigate the distribution of Wrch-1 relative to the AJ-associated proteins, β-catenin and E-cadherin. These proteins overlapped with Wrch-1 along the basolateral membrane (Fig. 3C and D, bottom *xz* panels) and along the PM at the apical and basal margins of the lateral membrane (Fig. 3C and D, top apical and basal panels). These data suggest a potential role for Wrch-1 in regulating the structure and function of AJC by modulating cell junctions (both TJs and AJs), which are required for proper epithelial cell morphology.

Activated Wrch-1 disrupts TJ formation during cell polarization. Rho GTPases regulate the formation and maintenance of both TJs and AJs (11, 41). Wrch-1 distribution to cell-cell junctions and its association with the TJ-associated protein Par6 suggest that Wrch-1 could regulate TJ formation and function. Therefore, we generated a large panel of MDCKII epithelial cells stably expressing HA-tagged Wrch-1 proteins (Fig. 4A) and used confocal microscopy to investigate the localization of TJ proteins during calcium-induced cell polarization in the presence or absence of activated Wrch-1. Briefly, culturing cells in calcium-depleted medium disrupts cell-cell contacts, and junction proteins are internalized in cytosolic vesicles. Restoration of calcium (calcium switch) triggers TJ assembly and cell polarization in a series of kinetically regulated steps. In the absence of calcium (Fig. 4B, 0 h), the TJ-associated protein ZO-1 was normally localized to a diffuse perinuclear ring structure that is enriched in actin filaments (43). Following calcium switch, ZO-1 was redistributed to the lateral surface of the newly formed cell-cell contacts (Fig. 4B,

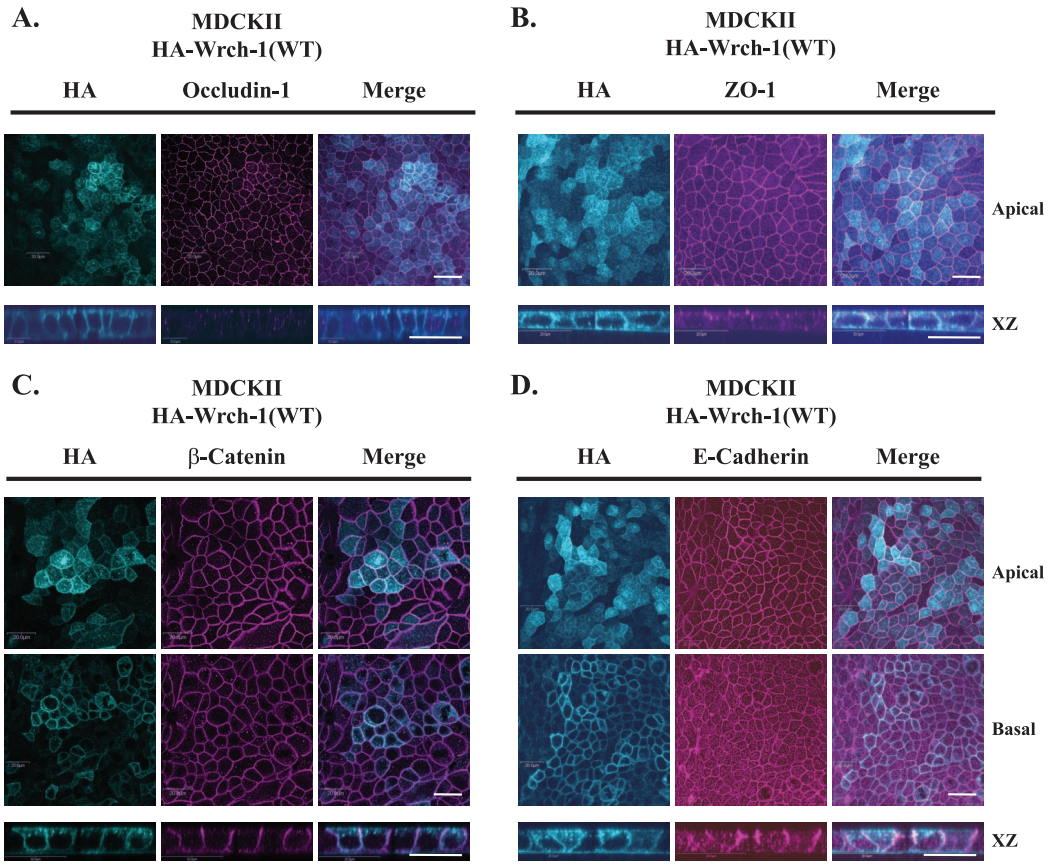

FIG. 3. Wrch-1 localizes to cell junctions in polarized MDCK cells. Cells were grown to confluence as described above and then fixed and probed for the HA epitope tag (cyan) and either occludin (magenta) (A), ZO-1 (magenta) (B), β-catenin (magenta) (C), or E-cadherin (magenta) (D). Square panels, *xy* sections; rectangular panels, *xz* sections (top to bottom). Scale bars, 20 μm.

12 h) in both control cells and cells expressing WT Wrch-1. This redistribution of ZO-1 is consistent with the formation of normal TJs.

Strikingly, in cells expressing activated Wrch-1(Q107L), the diffuse perinuclear accumulation of ZO-1 was missing in the absence of cell-cell contacts (Fig. 4B, 0 h). Furthermore, following readdition of calcium the movement of ZO-1 to the AJC was significantly delayed, as indicated by lack of ZO-1 at the apical surface, and the distribution of ZO-1 within the AJC at later time points (Fig. 4B, 12 h) was disorganized relative to cells expressing vector only or WT Wrch-1. This mislocalization of ZO-1 is consistent with a delay in proper TJ formation. However, ZO-1 eventually localized properly to TJs in these monolayers after 5 days (data not shown), suggesting that it is the kinetics of TJ formation, and not maintenance of TJ structure in polarized cells, that is altered by activated Wrch-1.

Activated Wrch-1 disrupts TJ integrity during cell polarization. The physiological function of TJs, known as the "gate" function (23), is to form a barrier to the movement of ions and solutes between cells. The formation of this barrier over time can be measured by the development of TER, and is a functional measure of TJ assembly. To investigate the role of Wrch-1 in normal TJ "gate" function, we measured TER development in MDCKII cells after calcium switch. In cells expressing empty vector or WT Wrch-1, TER increased linearly, reaching an initial peak value at ~18 h before falling to steady-state levels. In contrast, cells expressing activated Wrch-1(Q107L) or Wrch-1(ΔN-Q107L) demonstrated altered TER development, displaying a threefold reduction in peak resistance at 18 h (Fig. 4C). However, the rate of TER development was unaffected, and steady-state TER levels were identical in all cell lines by 80 h. Interestingly, expression of an activated form of Wrch-1 that is mislocalized to the cytosol due to mutational loss of its C-terminal palmitoylation site, Wrch-1(Q107L/SSFV), did not delay TER development (Fig. 4C), suggesting that proper membrane localization of Wrch-1 is required for its ability to modulate the TJ "gate" function.

Significantly, expression of active, GTP-bound Wrch-1 did not prevent the eventual formation of a functional TJ seal by ~18 h, as indicated by resistance measures above 800 $\Omega \times cm^2$. This is in contrast to constitutively active Ras, which is known to disrupt cell junctions entirely (25) (Fig. 4C). These data show that enhanced Wrch-1 activity disrupts TJ "gate" function only during early TJ assembly, whereas steady state TJ permeability is unaffected.

The "gate" formed by TJs is not only selectively permeable to ion flow but also regulates the paracellular flux of hydrophilic uncharged molecules. Thus, we measured the paracellular diffusion of FITC-conjugated dextran tracer molecules of 4,000 kDa and 40,000 kDa across cell monolayers. Tracer dif-

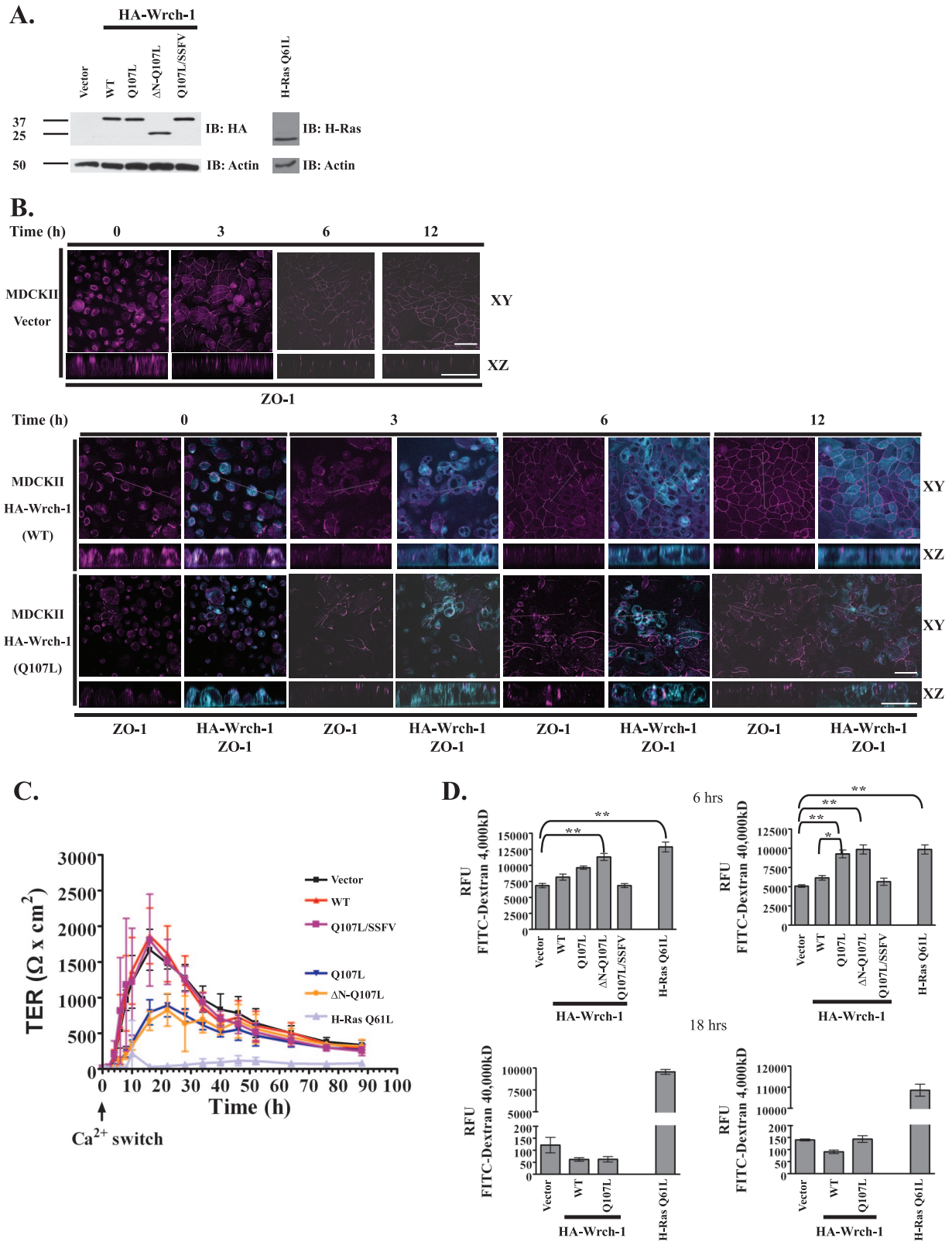

FIG. 4. Activated Wrch-1 disrupts TJ formation and integrity during cell polarization. (A) Equivalent expression in MDCKII cells of indicated HA-tagged Wrch-1 constructs and H-Ras(Q61L) shown by immunoblot (IB) with anti-HA and anti-Ras antibodies. The loading control was anti-β-actin. (B) MDCKII cells stably expressing empty vector or HA-tagged Wrch-1 were grown on 12-mm Transwell filters and subjected to calcium switch. Cells were fixed at the indicated intervals and stained using primary antibodies against the HA epitope tag (cyan) and ZO-1 (magenta). Square panels, *xy* sections; rectangular panels, *xz* sections (top to bottom). Scale bars, 20 μm. (C) Cells were subjected to calcium switch as in panel B. At indicated time points after calcium readdition, TER ($\Omega \times cm^2$) was measured using an epithelial volt-ohmmeter. (D) Cells were

fusion was evaluated 6 h after induction of cell-cell contacts by the addition of calcium to the apical surface of confluent cell monolayers grown on filters. As expected, there was minimal difference in the transcellular diffusion of either tracer in cells expressing WT Wrch-1 compared to empty vector control cells. In contrast, we observed a significant enhancement in the diffusion of both dextrans in cells expressing activated Wrch-1 or Ras (Fig. 4D). As in the TER experiments, the nonpalmitoylated cytosolic mutant of activated Wrch-1(Q107L/SSFV) did not produce an increase in paracellular flux (Fig. 4D). Similarly, dextran flux in cells expressing activated Wrch-1 was ultimately normal at ~18 h after calcium switch (Fig. 4D). Taken together, these data suggest that aberrant activation of Wrch-1 leads to disruption of early events in TJ assembly and that other cellular mechanisms capable of regulating TJ dynamics compensate at later time points to form a functional TJ.

Activated Wrch-1 disrupts actin organization during cell polarization and overall cell morphology of MDCKII cells. There is an intimate relationship between the actin cytoskeleton, cell junctions, and epithelial morphogenesis. The dynamic reorganization of F-actin is closely correlated with changes in cell structure and the regulation of junction assembly. The loss of ZO-1-associated perinuclear actin filaments during early junction assembly led us to hypothesize that Wrch-1 may regulate actin dynamics during polarization of epithelial cells. To address this hypothesis, we examined actin organization in monolayers of cells stably expressing empty vector, WT Wrch-1, or Wrch-1(Q107L) following calcium switch. As previously described, in the absence of cell-cell contact, we observed a diffuse cytosolic ring of actin filaments at the apical surface of MDCKII cells expressing vector or WT Wrch-1 (Fig. 5A, 0 h). This structure was absent in cells expressing activated Wrch-1(Q107L), and the actin staining was distributed diffusely throughout the cytosol (Fig. 5A, 0 h). After addition of calcium, the perinuclear actin ring redistributed toward the PM in cells expressing vector or WT Wrch-1 (Fig. 5A, 15 min) and subsequently accumulated at cell-cell contacts, as evident by the intense actin staining between cells (Fig. 5A, 30 min). In contrast, cells expressing activated Wrch-1(Q107L) still lacked an actin-rich ring structure, and displayed an apparent decreased density of F-actin at the center and periphery (Fig. 5A, 15 and 30 min). Furthermore, F-actin accumulation at cell-cell contacts was delayed (Fig. 5A, 1 h). These results suggest that proper cycling of Wrch-1 is required to regulate cytoskeletal dynamics during junction assembly in epithelia.

These observations led us to examine whether activated Wrch-1 disrupts normal epithelial cell morphology in monolayer culture. Normal monolayers are composed of cuboidal, columnar epithelial cells with actin-rich microvilli, a contractile ring of F-actin at the AJC, a cortical array of short actin filaments on the lateral domain, and actin stress fibers at the basal surface. Epithelial cells expressing vector or WT Wrch-1 formed normal monolayers of tightly packed cuboidal cells, and F-actin accumulated in basal stress fibers and within the AJC. In contrast, cells expressing activated Wrch-1 were squamous, multilayered, and in general more disorganized within the monolayer (Fig. 5B). This loss of normal cell morphology was accompanied by the disruption of perijunctional actin bundles normally associated with the AJC (Fig. 5B, apical) and by disruption of the basal stress fibers (Fig. 5B, basal). Together, these data show that expression of activated Wrch-1 disrupts normal epithelial cell morphogenesis and that this loss of normal cell morphology could be mediated by Wrch-1 modulation of the actin cytoskeleton.

Coordinate regulation of Wrch-1 binding to Par6 and disruption of TJs and actin organization during cell polarization. To determine if the ability of Wrch-1 to disrupt TJ dynamics and actin organization was linked to the GTP-dependent interaction between Wrch-1 and Par6, we performed site-directed mutagenesis within the effector domain of Wrch-1 to create a mutant incapable of binding Par6. Previous mutational analysis of Cdc42 identified a single point mutation at Tyr40 in the effector domain that was capable of blocking the interaction of active Cdc42-GTP with the CRIB-PDZ cassette of Par6 (13). Therefore, we constructed a point mutation at the analogous residue of Wrch-1, F86C, to test whether this mutation would abrogate the GTP-dependent interaction of Wrch-1 and Par6. Unlike the HA-tagged parental Wrch-1(Q107L), the effector domain mutant (EDM) Wrch-1(Q107L/F86C) did not interact with GST-Par6 or immunoprecipitated Myc-Par6 (Fig. 6A and B), as predicted by analogy to the Cdc42 EDM.

We then generated MDCKII cells stably expressing the Wrch-1 EDM (Fig. 6C) to test the requirement for Par6 or other CRIB domain-containing proteins in Wrch-1-mediated modulation of TJ assembly and cytoskeletal dynamics. We observed that the Wrch-1 EDM did not interfere with correct localization of ZO-1 during calcium-induced cell polarization (Fig. 6D). Further, Wrch-1 EDM localization (Fig. 6D) was distinct from that of activated Wrch-1(Q107L) and instead resembled that of WT Wrch-1 (Fig. 4B). Expression of the activated Wrch-1 EDM was also unable to delay initial TER development (Fig. 6E). Finally, we observed that calcium-induced redistribution of F-actin in the EDM mutant from the perinuclear network to the AJC was indistinguishable from WT Wrch-1 (Fig. 6F). These data suggest that the interaction between Wrch-1 and Par6 may contribute to the localization of active GTP-bound Wrch-1 and the regulation of TJ assembly and cytoskeletal dynamics.

Activated Wrch-1 disrupts epithelial morphogenesis and promotes anchorage-independent growth of MDCKII cells. Recent studies have highlighted the utility of 3D culture systems for analysis of epithelial cell polarity and morphology because they mimic the in vivo formation of epithelial structures (32, 50). For example, MDCK cells grown in extracellular matrix form highly polarized structures known as "cysts," composed of polarized cells whose apical domains surround a hol-

subjected to calcium switch as in panel B. Paracellular flux of 4,000-kDa FITC-dextran (FD-4) or 40,000-kDa FITC-dextran (FD-40) tracer was examined 6 h and 18 h after calcium switch. RFU, relative fluorescence units. Bar graphs represent an average of three independent experiments carried out in triplicate for each cell line ± standard error of the mean. Significant P values of <0.01 or <0.001 are indicated by * or **, respectively. Tukey's multiple comparison test was used to determine significance between cell lines.

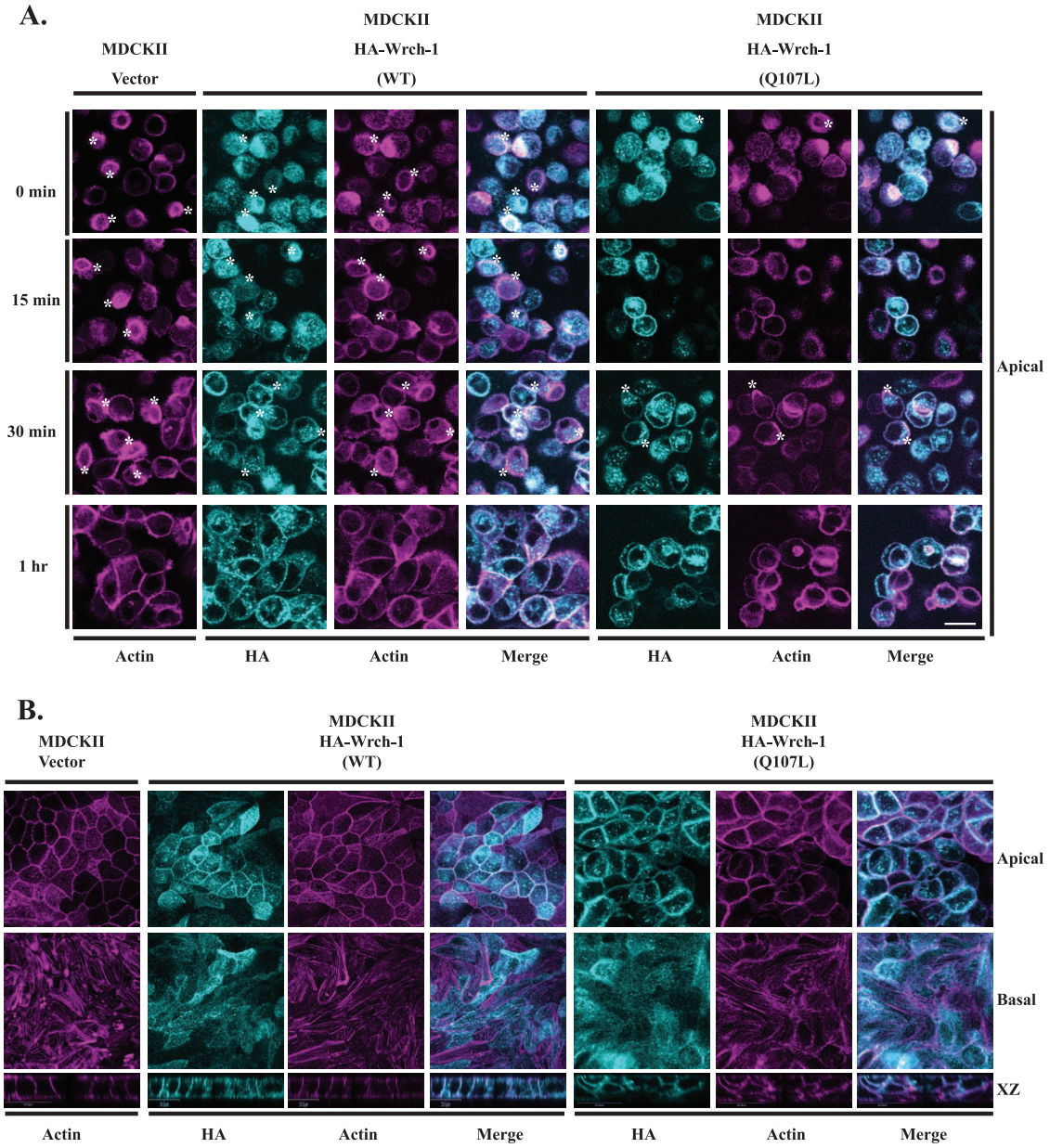

FIG. 5. Activated Wrch-1 disrupts actin organization and cell morphology of MDCKII cells. (A) MDCKII cells stably expressing empty vector or the indicated HA-tagged Wrch-1 constructs were subjected to calcium switch and treated as in Fig. 4B, including probing for the HA epitope tag (cyan) or with Texas Red-phalloidin (magenta). Asterisks represent actin contractile rings and sites of cell-cell contact. (B) Cells as in panel A were grown to confluence on 12-mm Transwell filters and then fixed, stained, probed for the HA epitope tag (cyan) or with Texas Red-phalloidin (red), and visualized by confocal microscopy. Square panels, *xy* sections; rectangular panels, *xz* sections (top to bottom). Scale bars, 20 μm.

low lumen. To investigate the role of Wrch-1 proteins in epithelial morphogenesis, we grew MDCKII cells in a matrix of collagen I. Monodispersed cells were grown for 10 days until they developed into cysts. These cysts were examined using IF directed against apical and basal polarity determinants such as ZO-1 and E-cadherin to determine whether apicobasal polarity was established. Cells expressing empty vector or WT Wrch-1 formed multicellular cysts with a single luminal space and polarized membrane domains in which ZO-1 was sequestered at the apical membrane and E-cadherin along the lateral membrane (Fig. 7A). In contrast, cysts formed by cells expressing activated Wrch-1 contained either multiple minilumens or no lumen at all. However, individual cells within these highly disorganized cysts nevertheless retained proper apicobasal polarity, with ZO-1 sequestered toward the center and E-cadherin localized to the outside of the cysts. Importantly, expression of the active Wrch-1 mutant that lacks proper membrane localization did not disrupt normal epithelial cell polarity. These data suggest that proper epithelial morphogenesis in 3D requires spatial and/or temporal regulation of Wrch-1 activity.

We next attempted to quantify the degree of cyst lumen development. In normal cysts, cortical actin staining outlines

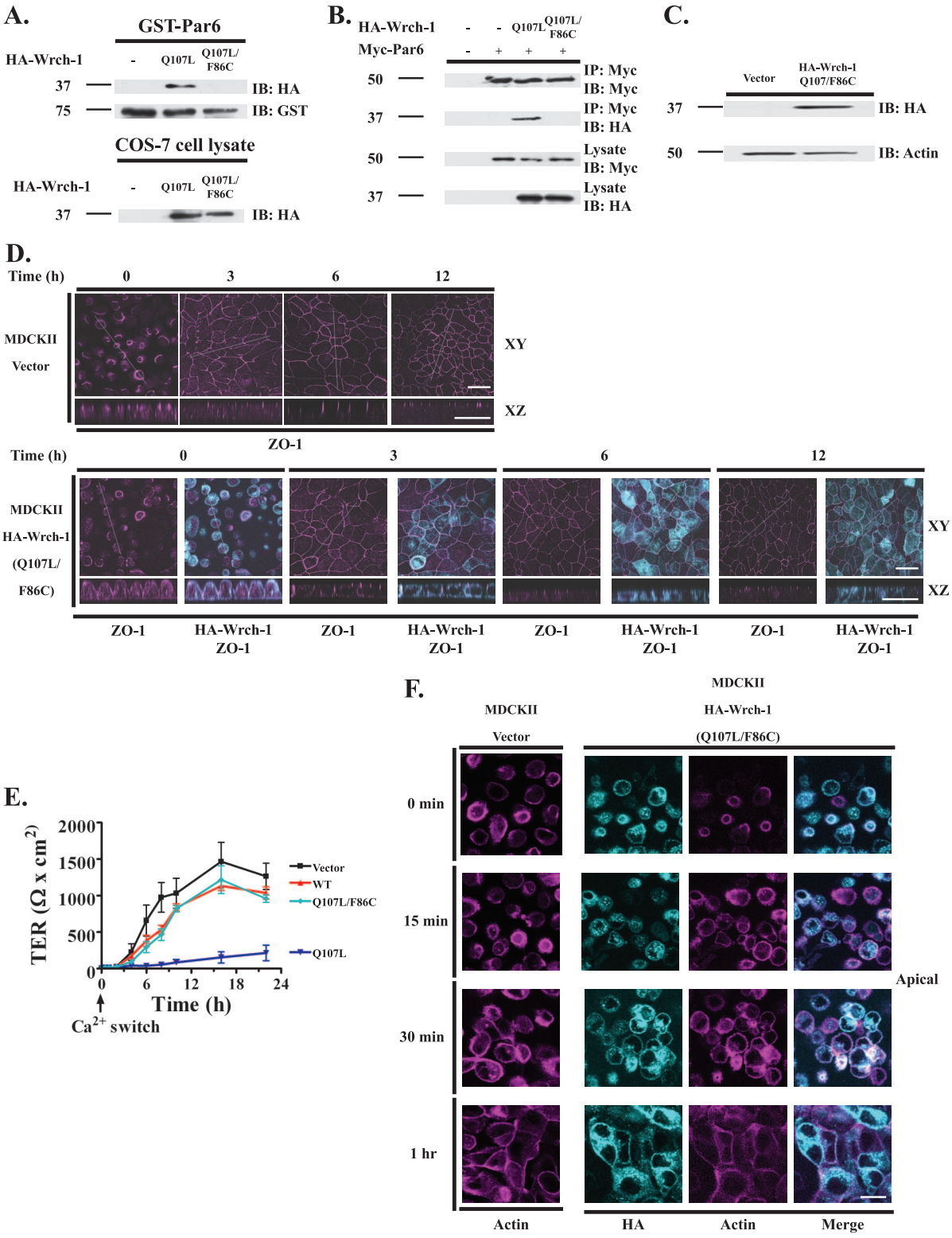

FIG. 6. An effector domain mutation in Wrch-1 abrogates Par6-binding and its ability to disrupt TJ formation and actin organization during cell polarization. (A) Lysates from COS-7 cells transiently expressing the indicated constructs including the EDM Wrch-1(Q107L F86C) were subjected to GST pulldowns as in Fig. 1A. IB, immublotting. (B) Lysates from COS-7 cells expressing the indicated constructs were subjected to coimmunoprecipitation and immunoblotting as in Fig. 1B. (C) Stable expression in MDCKII cells of HA-tagged Wrch-1(Q107L F86C) was detected by immunoblotting with anti-HA antibody. Anti-β-actin was used as a loading control. (D) MDCKII cells stably expressing empty vector or Wrch-1(Q107L F86C) were subjected to calcium switch, and the localization of Wrch-1 (cyan) and ZO-1 (magenta) was evaluated as in Fig. 4B. Square panels, *xy* sections; rectangular panels, *xz* sections (top to bottom). Scale bars, 20 μm. (E) TER (Ω × cm^2) was measured in cells subjected to calcium switch, at indicated time points after calcium readdition. (F) Actin organization was evaluated in cells expressing vector only or EDM Wrch-1 and subjected to calcium switch. Cells were fixed at indicated intervals after readdition of calcium and stained using either anti-HA antibody (cyan) or Texas Red-phalloidin (magenta). Asterisks represent actin contractile rings and sites of cell-cell contact.

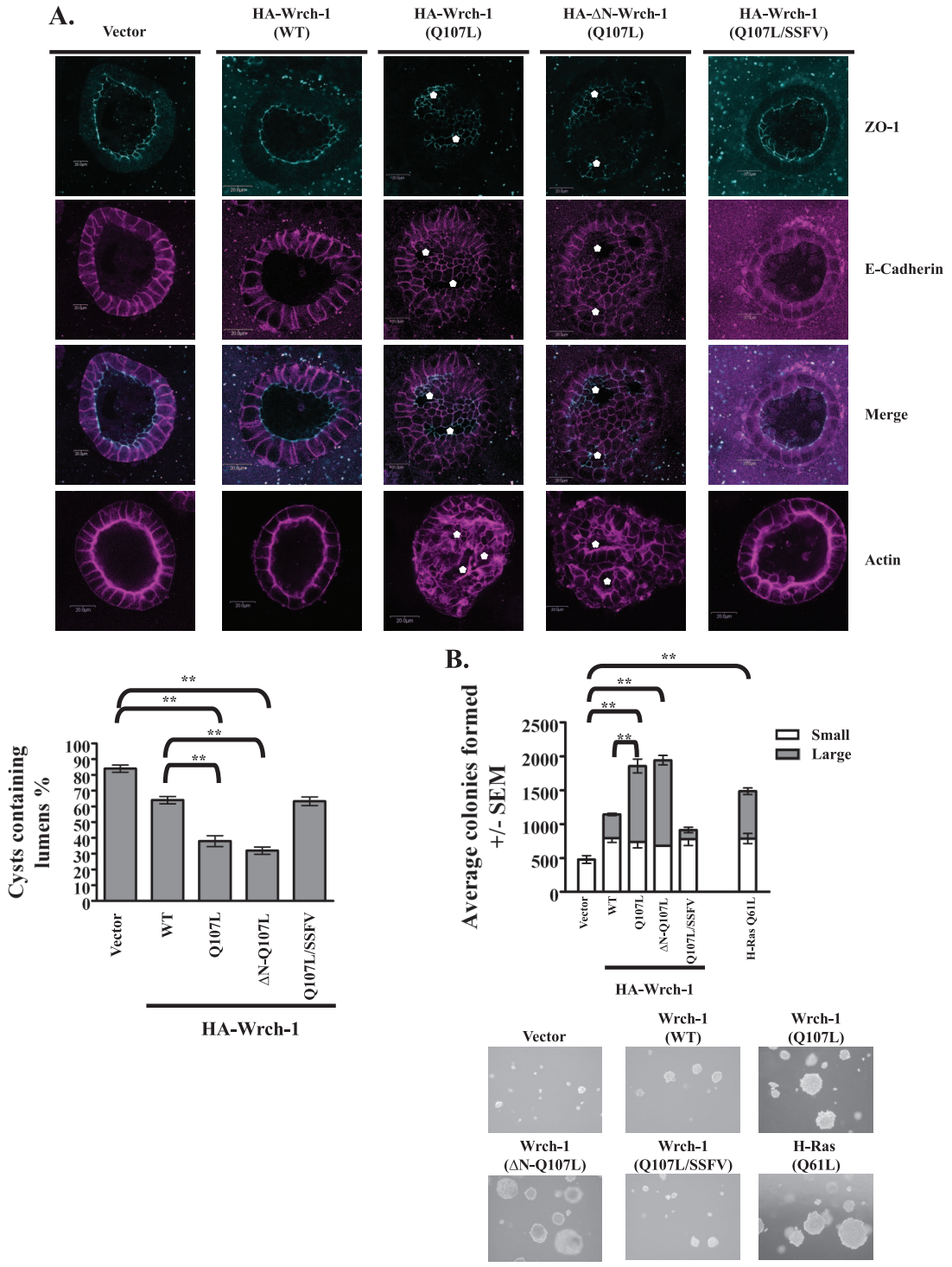

FIG. 7. Activated Wrch-1 disrupts epithelial morphogenesis and promotes anchorage-independent growth of MDCKII cells. (A) MDCKII cells stably expressing empty vector or indicated HA-tagged Wrch-1 constructs were grown in collagen I gels. After 10 days, collagen gels were fixed and stained for ZO-1 (cyan) and E-cadherin (magenta) (top panels) to examine epithelial cell polarity or with Texas Red-phalloidin (magenta) (bottom panel) to examine epithelial morphogenesis and lumen formation. Scale bars, 20 μm. Cysts containing a single lumen were quantified by counting cysts with single luminal area as positive and cysts with no lumen as negative. Bar graphs represent an average of three independent experiments carried out in triplicate for each cell line ± the standard error of the mean (SEM). Tukey's multiple comparison test was used to determine significance between cell lines. Significant P values of <0.001 are indicated by **. (B) Anchorage-independent growth. MDCKII cells were seeded into soft agar and analyzed for their ability to induce colony formation. Colonies formed after 14 days were stained and scanned, and the numbers of small (6 to 15 cells across) and large (>15 cells across) colonies were quantified. Images and bar graphs are representative of three separate experiments carried out in triplicate; shown are averages ± SEM. Significant P values of <0.001, obtained by using Tukey's multiple comparison test, are indicated by **.

the cell periphery. Cysts expressing activated Wrch-1 did not contain defects in the formation of the cortical actin cytoskeleton. However, the absence of a luminal structure or the formation of multiple lumens was easily visualized upon staining these cysts with Texas Red-phalloidin (Fig. 7A). We determined that the formation of cysts with a single luminal space was abrogated by two- to threefold upon expression of activated Wrch-1 and that proper membrane localization was required for this observation. These data highlight that proper regulation of Wrch-1 activity is necessary for normal epithelial morphogenesis in 3D and outline a potential mechanism for Wrch-1-mediated transformation.

The loss of epithelial cell morphogenesis due to the disruption of cell junctions is a characteristic of cellular transformation. Therefore, we next examined the ability of Wrch-1 to induce anchorage-independent growth, another hallmark of transformation, by assessing the ability of MDCKII cells stably expressing Wrch-1 proteins to form colonies in soft agar. We observed that WT Wrch-1 induced twice as many colonies as empty vector (Fig. 7B). As predicted, activated full-length and N-terminally truncated Wrch-1 were more potently transforming than WT Wrch-1, inducing colony numbers fourfold over empty vector controls (Fig. 7B), and those colonies were substantially larger in size than those induced by WT Wrch-1. These data demonstrate that Wrch-1 activity promotes anchorage-independent growth. We hypothesize that the difference in colony size observed between WT and constitutively activated forms of Wrch-1 is due to disruption of actin organization and cell-cell contacts by the latter.

The effector domain mutation that blocks Par6 binding abrogates Wrch-1-mediated disruption of epithelial morphogenesis and partially impairs anchorage-independent growth. We hypothesized that the Par6-binding-deficient EDM that failed to disrupt actin organization or perturb TJs would also be incapable of disrupting epithelial morphogenesis. In cysts grown in 3D collagen from cells expressing vector or Wrch-1(Q107L F86C), epithelial morphogenesis was intact (Fig. 8A) and ZO-1 was sequestered at the apical surface facing the lumen, while E-cadherin was localized to the basolateral membrane. These results indicate that Wrch-1-mediated disruption of epithelial morphogenesis (e.g., Fig. 7A) requires the binding of a CRIB domain-containing effector such as Par6.

The inability of the EDM to misregulate epithelial morphogenesis led us to investigate whether it retained the ability to induce anchorage-independent growth. Interestingly, this EDM was only partially defective in growth transformation. Cells expressing Wrch-1(Q107L F86C) formed small or large colonies similar to those formed by WT-expressing cells (Fig. 8B) and did not show the increased number of large colonies characteristic of activated Wrch-1. These data suggest that formation of the large colonies induced by expression of active, constitutively GTP-bound Wrch-1 requires another effector whose binding is not perturbed by the F86C mutation that impairs Par6 interaction.

Loss of Wrch-1 expression perturbs epithelial morphogenesis. We have shown here that ectopic expression of a constitutively active mutant of Wrch-1(Q107L) in MDCKII cells disrupts TJ dynamics, cytoskeletal organization, and morphogenesis and that this disruption represents a potential mechanism by which excess Wrch-1 activity mediates cellular trans-

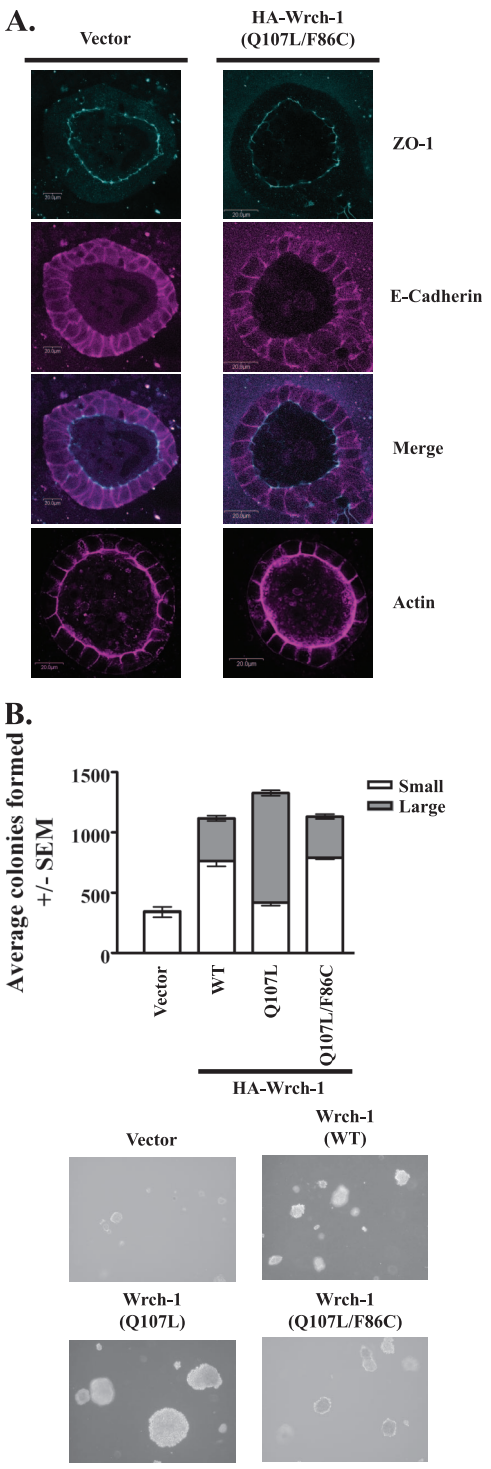

FIG. 8. Effector domain mutation in Wrch-1 abrogates Wrch-1-mediated disruption of epithelial morphogenesis and promotion of anchorage-independent growth of MDCKII cells. (A) MDCKII cells stably expressing empty vector or HA-tagged Wrch-1(Q107L F86C) were treated and evaluated as in Fig. 7A. (B) MDCKII cells stably expressing empty vector, WT Wrch-1, Wrch-1(Q107L), or Wrch-1(Q107L F86C) were seeded into soft agar and analyzed for their ability to induce anchorage-independent growth as indicated in Fig. 7B. SEM, standard error of the mean.

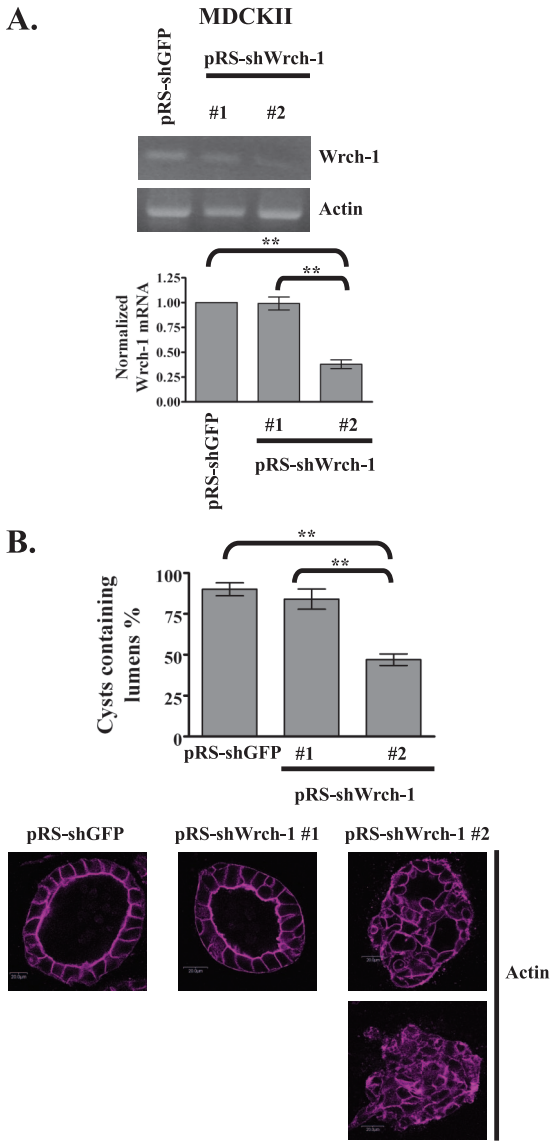

FIG. 9. Loss of Wrch-1 expression perturbs epithelial morphogenesis. (A) mRNA levels of Wrch-1 or actin isolated from MDCKII cells stably expressing pRS-GFP, pRS-shWrch-1 no. 1 or pRS-shWrch-1 no. 2. Quantification of Wrch-1 mRNA levels was normalized to actin using ImageJ. Bar graphs represent an average of three independent experiments for each cell line ± the standard error of the mean (SEM). Tukey's multiple comparison test was used to determine significance between cell lines. Significant P values of <0.001 are indicated by **. (B) MDCKII cells stably expressing pRS-GFP, pRS-shWrch-1 no. 1, or pRS-shWrch-1 no. 2 were treated and evaluated as in Fig. 7A.

formation. To determine the extent to which endogenous Wrch-1 is required for normal processes such as epithelial morphogenesis, we generated MDCK II cell lines expressing Wrch-1-specific shRNAs to knock down expression of endogenous Wrch-1. A significant reduction (~65%) of Wrch-1 mRNA was observed upon the introduction of Wrch-1 shRNA no. 2 when compared to the negative control non-effective GFP-directed shRNA or to Wrch-1 shRNA no. 1, which did not effectively reduce Wrch-1 mRNA (Fig. 9A). Therefore, in the following experiments we used MDCKII cells expressing Wrch-1 shRNA no. 1 as an additional negative control. In cysts grown in 3D collagen from cells expressing GFP-directed shRNA or the ineffective Wrch-1 shRNA no. 1, in which endogenous Wrch-1 levels were unimpaired, epithelial morphogenesis occurred normally (Fig. 9B). In contrast, cysts formed by MDCKII cells in which endogenous Wrch-1 was reduced upon expression of Wrch-1 shRNA no. 2 had either no lumen or multiple small lumens (Fig. 9B). These data indicate that normal levels of endogenous Wrch-1 are required for normal epithelial morphogenesis in a 3D culture system capable of recapitulating the in vivo formation of epithelial structures.

DISCUSSION

Recent studies have described roles for the atypical Rho GTPase Wrch-1 in actin cytoskeletal organization (39), focal adhesion formation, and cell motility in nonepithelial cells (8, 30). In the present study, we demonstrate that Wrch-1 is required for normal epithelial morphogenesis in 3D culture. We have identified a novel biological function for Wrch-1 in regulating actin cytoskeletal reorganization that is necessary for proper epithelial morphogenesis and kinetics of TJ assembly. We hypothesize that the loss of epithelial morphogenesis seen here in the presence of excessive Wrch-1 activity contributes to the ability of constitutively active, GTP-locked Wrch-1 to induce transformation of epithelial cells.

Epithelial morphogenesis is a multistep process that requires regulated adhesion and coordinated cell shape changes within an epithelium. Proper modulation of the actin cytoskeleton is a critical component of these morphogenetic processes. It was shown previously that expression of activated Wrch-1 mediates actin stress fiber dissolution and cell rounding in fibroblasts (39). We have demonstrated here that activated Wrch-1 disrupts several distinct pools of F-actin during calcium-mediated polarization of MDCKII cells. First, we observed that the actin-rich perinuclear ring present in cells devoid of contact is missing in cells expressing activated Wrch-1. This structure redistributes to the PM during junction assembly and polarization and is believed to mediate the movement of junctional proteins from internal vesicles to the periphery of the cells (1, 40). Therefore, we hypothesize that it is the disruption of this cytoskeletal domain by activated Wrch-1 that disrupts early TJ assembly in MDCKII cells.

Regulation of actin cytoskeleton dynamics by Rho GTPases has been proposed as a general mechanism for regulation of TJ assembly during cell polarization (6, 26). Expression of constitutively activated, GTP-locked Wrch-1 disrupted TJ formation and integrity during cell polarization. Although the rate of TER development of activated Wrch-1-expressing monolayers was similar to that of control monolayers, the peak magnitude of TER was markedly reduced, by mechanisms that are currently unclear. However, TJs do form eventually in cells expressing activated Wrch-1, suggesting that initial regulation of Wrch-1 activation is necessary only for early TJ dynamics and not for TJ maintenance. These findings are strikingly similar to the kinetic delay in TJ formation following RNA interference-mediated knockdown of the tight junction scaffolding protein ZO-1 (24), where it was proposed that the loss of the perinu-

clear ring of actin in ZO-1 knockdown cells might inhibit the delivery of TJ-associated barrier proteins to the cell boundary.

Activated Wrch-1 also perturbed cytoskeletal organization in confluent monolayers. The sharp, linear band of actin associated with AJC and the basal stress fibers were highly disorganized in MDCKII cells expressing activated Wrch-1. These changes were accompanied by a dramatic alteration in the organization of these cells within the monolayer and by defects in cystogenesis of cells grown in 3D collagen matrix. These observations suggest that Wrch-1 may regulate cytoskeletal dynamics that underlie tissue morphogenesis in epithelia. It is not surprising that either constitutive activation or shRNA-mediated knockdown of Wrch-1 promotes the disruption of epithelial morphogenesis; rather, these findings are consistent with a requirement for tightly and correctly regulated Wrch-1 activity to support normal cystogenesis. A similar requirement for optimal levels of endogenous Cdc42 to promote proper cystogenesis has been observed in two independent studies that investigated the effect of RNA interference-mediated knockdown of Cdc42 or expression of constitutively active or dominant-negative Cdc42 (22, 34). In all cases, misregulation of Cdc42 resulted in the reduction of normal lumen-containing cysts, suggesting that tight regulation of members of the Rho GTPase family is necessary for normal epithelial cell morphogenesis.

Indeed, we had initially speculated that the identification of the polarity complex protein Par6 as a GTP-dependent binding partner of Wrch-1 suggested a possible role for Wrch-1 in modulating cell polarity. However, aberrant regulation of Wrch-1 activity does not affect cell polarity in 3D culture, suggesting that Wrch-1 interaction with the Par3-Par6-PKC ζ complex plays a distinct role from the previously described regulation by Cdc42. We previously showed that Cdc42 and Wrch-1 have distinct localizations in fibroblasts (5), and our present work also suggests that these related GTPases have divergent localizations in epithelial cells. For example, Cdc42 was shown to localize to the apical surface of MDCK cysts grown in 3D, and suppression of Cdc42 expression disrupted normal apicobasal polarity in 3D culture (22). This is distinct from the basolateral PM localization of Wrch-1 characterized in this report and our observation that activated Wrch-1 or reduction of Wrch-1 expression disrupts cell morphology and cystogenesis without perturbing apicobasal polarity. Therefore, we hypothesize that both Cdc42 and Wrch-1 regulate the Par3-Par6-PKC ζ complex, but at different spatial or temporal domains.

The loss of epithelial cell morphology is characteristic of dedifferentiated cancer cells that lose normal cell polarity and cell-cell contacts. Previous studies in this laboratory demonstrated that activated Wrch-1 promotes anchorage-independent growth of NIH 3T3 fibroblasts, a hallmark of oncogenic transformation (5, 42), and we have shown here that stable expression of activated Wrch-1 also promotes anchorage-independent growth of MDCKII epithelial cells. Recent studies have highlighted the ability of oncogenes to hijack cell polarity protein complexes to promote dedifferentiation in the early stages of epithelial cell carcinogenesis. The Par6-PKC ζ protein complex has been identified as a downstream player in the loss of cell polarity, in epithelial-mesenchymal transition, and in increased cell proliferation mediated by receptor tyrosine kinases, including ErbB2, and by transforming growth factor β, all of which promote cellular transformation and migration (2, 31). However, the exact mechanisms by which misregulation of cell polarity proteins leads to dedifferentiation and transformation remain to be determined. It has been shown previously that transformation mediated by aberrant activation of Cdc42 or Rac can be potentiated by the Par6-PKC ζ complex (33). These findings further support a link between the regulation of cell morphology by Rho GTPases and contact-inhibited growth.

Our data suggest that Par6 may be one important effector of activated Wrch-1 in epithelial morphogenesis. This hypothesis is supported in part by our observation that an EDM of activated Wrch-1 that cannot bind Par6 is unable to disrupt cell architecture and cyst formation in MDCKII cells. It is also supported by the previously published observations that alterations in Par6 expression have many of the same effects on epithelial morphogenesis as abnormal levels of Wrch-1 activity. For example, overexpression of Par6 delays TJ assembly in MDCKII cells (12), and expression of a dominant-negative form of Par6 in MDCK cells grown in collagen disrupts cystogenesis (19).

The most pressing question, then, is how the Wrch-1–Par6 effector complex regulates cytoskeletal dynamics. Chen et al. recently identified a link between the cell polarity protein Par3 and regulation of actin dynamics important for proper TJ assembly, in which Par3 binds to and inhibits LIMK activity, leading to a subsequent decrease in cofilin activity (7). Therefore, we predict that the association between active Wrch-1 and the Par3-Par6-PKC ζ complex may ultimately alter actin dynamics through known Rho GTPase effectors such as LIMK.

Despite the similarity in the epithelial phenotypes generated by Par-6 and Wrch-1 mutations, it is still possible that other Wrch-1 effectors may be involved. At present, the only other proteins identified to date whose properties are consistent with an effector function for Wrch-1 are PAK1 (8, 39) and Pyk2 (37). Pyk2 is a Wrch-1 effector capable of mediating Wrch-1 effects on cytoskeletal dynamics of filopodia and stress fibers. Pyk2 could represent a relevant effector for Wrch-1-mediated defects in cystogenesis, because the single F86C point mutation in Wrch-1 was sufficient to block its interaction with Pyk2 or to abolish Wrch-1-mediated loss of stress fibers or formation of filopodia (37). Unlike Pyk2, the interaction between Wrch-1 and Pak1 is not abrogated by the F86C point mutation, suggesting that Pak1 may not contribute to the biological activities revealed in this study (30). Understanding the exact mechanisms whereby Wrch-1 regulates each of these distinct processes will likely require further investigation of known Wrch-1 effector targets as well as identification of novel Wrch-1 effectors.

However, the F86C EDM of Wrch-1 that is incapable of interacting with Par6 nevertheless retains the ability to weakly promote anchorage-independent growth, suggesting that other Wrch-1 effectors must also contribute to Wrch-1-mediated transformation. As stated above, the interaction between Wrch-1 and Pak1 is not abrogated by this mutation (30), suggesting that the known interaction with Pak1 may contribute to Wrch-1-mediated transformation while the activity of Par6 is more restricted to morphogenesis. Of these two effectors, only Pak1 has been implicated in promoting anchorage-indepen-

dent growth (46), and it has been shown to be altered in human cancers (47). Whether Wrch-1 signaling through Pak1 could contribute to Wrch-1-mediated transformation bears further investigation.

Our observations that Wrch-1 can interact with the Par6-associated polarity complex and can disrupt epithelial cell morphology and cell junctions in a manner that can be abrogated by blocking Par6 binding suggest a potential mechanism for Wrch-1-mediated transformation. The identification of the gene coding for Wrch-1 as a gene whose expression is regulated by Wnt-1 signaling in mouse mammary epithelial cells and its ability to phenocopy Wnt-1 mediated transformation, along with aberrant regulation of Wrch-1 expression in various cancers, suggest the possibility that Wrch-1 may play a role in human tumorigenesis. Although naturally occurring activating mutations that lock Wrch-1 in the GTP-bound state have not been identified, the considerable evidence for a role for other Rho family GTPases in pathological states also does not include the discovery of activating mutations in the Rho proteins themselves but instead involves aberrant activity of their regulators, the guanine exchange factors and GTPase-activating proteins that modulate GTP/GDP cycling. Thus, further identification of its upstream activators, downstream negative regulators and effector targets will be critical for a fuller understanding of the molecular mechanisms and role of Wrch-1 in transformation.

ACKNOWLEDGMENTS

We thank Victoria Bautch (UNC-CH) for antibodies, Christopher Johnston (UNC-CH) for assistance with protein purification, and Sam Wolff (UNC-CH) for guidance in IF and TER experiments.

This work was supported by National Institutes of Health grants to A.D.C. (CA109550) and to A.S.F. and James M. Anderson (DK61397). J.K.A. was supported by NIH training grant T32-GM008581, and D.C.B. was supported by NIH training grants T32-GM007040 and T32-CA071341.

REFERENCES

1. **Ando-Akatsuka, Y., S. Yonemura, M. Itoh, M. Furuse, and S. Tsukita.** 1999. Differential behavior of E-cadherin and occludin in their colocalization with ZO-1 during the establishment of epithelial cell polarity. J. Cell. Physiol. **179:**115–125.
2. **Aranda, V., T. Haire, M. E. Nolan, J. P. Calarco, A. Z. Rosenberg, J. P. Fawcett, T. Pawson, and S. K. Muthuswamy.** 2006. Par6-aPKC uncouples ErbB2 induced disruption of polarized epithelial organization from proliferation control. Nat. Cell Biol. **8:**1235–1245.
3. **Aronheim, A., Y. C. Broder, A. Cohen, A. Fritsch, B. Belisle, and A. Abo.** 1998. Chp, a homologue of the GTPase Cdc42Hs, activates the JNK pathway and is implicated in reorganizing the actin cytoskeleton. Curr. Biol. **8:**1125–1128.
4. **Aspenstrom, P., A. Fransson, and J. Saras.** 2004. Rho GTPases have diverse effects on the organization of the actin filament system. Biochem. J. **377:** 327–337.
5. **Berzat, A. C., J. E. Buss, E. J. Chenette, C. A. Weinbaum, A. Shutes, C. J. Der, A. Minden, and A. D. Cox.** 2005. Transforming activity of the Rho family GTPase, Wrch-1, a Wnt-regulated Cdc42 homolog, is dependent on a novel carboxyl-terminal palmitoylation motif. J. Biol. Chem. **280:**33055–33065.
6. **Bruewer, M., A. M. Hopkins, M. E. Hobert, A. Nusrat, and J. L. Madara.** 2004. RhoA, Rac1, and Cdc42 exert distinct effects on epithelial barrier via selective structural and biochemical modulation of junctional proteins and F-actin. Am. J. Physiol. Cell Physiol. **287:**C327–C335.
7. **Chen, X., and I. G. Macara.** 2005. Par-3 controls tight junction assembly through the Rac exchange factor Tiam1. Nat. Cell Biol. **7:**262–269.
8. **Chuang, Y. Y., A. Valster, S. J. Coniglio, J. M. Backer, and M. Symons.** 2007. The atypical Rho family GTPase Wrch-1 regulates focal adhesion formation and cell migration. J. Cell Sci. **120:**1927–1934.
9. **Ellenbroek, S. I., and J. G. Collard.** 2007. Rho GTPases: functions and association with cancer. Clin. Exp. Metastasis **24:**657–672.
10. **Etienne-Manneville, S., and A. Hall.** 2002. Rho GTPases in cell biology. Nature **420:**629–635.
11. **Fujita, Y., and V. Braga.** 2005. Epithelial cell shape and Rho small GTPases. Novartis Found. Symp. **269:**144–158, 223–230.
12. **Gao, L., G. Joberty, and I. G. Macara.** 2002. Assembly of epithelial tight junctions is negatively regulated by Par6. Curr. Biol. **12:**221–225.
13. **Garrard, S. M., C. T. Capaldo, L. Gao, M. K. Rosen, I. G. Macara, and D. R. Tomchick.** 2003. Structure of Cdc42 in a complex with the GTPase-binding domain of the cell polarity protein, Par6. EMBO J. **22:**1125–1133.
14. **Goldstein, B., and I. G. Macara.** 2007. The PAR proteins: fundamental players in animal cell polarization. Dev. Cell **13:**609–622.
15. **Izumi, Y., T. Hirose, Y. Tamai, S. Hirai, Y. Nagashima, T. Fujimoto, Y. Tabuse, K. J. Kemphues, and S. Ohno.** 1998. An atypical PKC directly associates and colocalizes at the epithelial tight junction with ASIP, a mammalian homologue of Caenorhabditis elegans polarity protein PAR-3. J. Cell Biol. **143:**95–106.
16. **Jaffe, A. B., and A. Hall.** 2005. Rho GTPases: biochemistry and biology. Annu. Rev. Cell Dev. Biol. **21:**247–269.
17. **Joberty, G., C. Petersen, L. Gao, and I. G. Macara.** 2000. The cell-polarity protein Par6 links Par3 and atypical protein kinase C to Cdc42. Nat. Cell Biol. **2:**531–539.
18. **Johansson, A., M. Driessens, and P. Aspenstrom.** 2000. The mammalian homologue of the Caenorhabditis elegans polarity protein PAR-6 is a binding partner for the Rho GTPases Cdc42 and Rac1. J. Cell Sci. **113:**3267–3275.
19. **Kim, M., A. Datta, P. Brakeman, W. Yu, and K. E. Mostov.** 2007. Polarity proteins PAR6 and aPKC regulate cell death through GSK-3beta in 3D epithelial morphogenesis. J. Cell Sci. **120:**2309–2317.
20. **Kirikoshi, H., and M. Katoh.** 2002. Expression of WRCH1 in human cancer and down-regulation of WRCH1 by beta-estradiol in MCF-7 cells. Int. J. Oncol. **20:**777–783.
21. **Lecuit, T., and P. F. Lenne.** 2007. Cell surface mechanics and the control of cell shape, tissue patterns and morphogenesis. Nat. Rev. Mol. Cell Biol. **8:**633–644.
22. **Martin-Belmonte, F., A. Gassama, A. Datta, W. Yu, U. Rescher, V. Gerke, and K. Mostov.** 2007. PTEN-mediated apical segregation of phosphoinositides controls epithelial morphogenesis through Cdc42. Cell **128:**383–397.
23. **Matter, K., and M. S. Balda.** 2003. Signalling to and from tight junctions. Nat. Rev. Mol. Cell Biol. **4:**225–236.
24. **McNeil, E., C. T. Capaldo, and I. G. Macara.** 2006. Zonula occludens-1 function in the assembly of tight junctions in Madin-Darby canine kidney epithelial cells. Mol. Biol. Cell **17:**1922–1932.
25. **Mullin, J. M., J. M. Leatherman, M. C. Valenzano, E. R. Huerta, J. Verrechio, D. M. Smith, K. Snetselaar, M. Liu, M. K. Francis, and C. Sell.** 2005. Ras mutation impairs epithelial barrier function to a wide range of nonelectrolytes. Mol. Biol. Cell **16:**5538–5550.
26. **Nusrat, A., M. Giry, J. R. Turner, S. P. Colgan, C. A. Parkos, D. Carnes, E. Lemichez, P. Boquet, and J. L. Madara.** 1995. Rho protein regulates tight junctions and perijunctional actin organization in polarized epithelia. Proc. Natl. Acad. Sci. USA **92:**10629–10633.
27. **Nusrat, A., C. von Eichel-Streiber, J. R. Turner, P. Verkade, J. L. Madara, and C. A. Parkos.** 2001. *Clostridium difficile* toxins disrupt epithelial barrier function by altering membrane microdomain localization of tight junction proteins. Infect. Immun. **69:**1329–1336.
28. **O'Brien, L. E., T. S. Jou, A. L. Pollack, Q. Zhang, S. H. Hansen, P. Yurchenco, and K. E. Mostov.** 2001. Rac1 orientates epithelial apical polarity through effects on basolateral laminin assembly. Nat. Cell Biol. **3:**831–838.
29. **O'Brien, L. E., W. Yu, K. Tang, T. S. Jou, M. M. Zegers, and K. E. Mostov.** 2006. Morphological and biochemical analysis of Rac1 in three-dimensional epithelial cell cultures. Methods Enzymol. **406:**676–691.
30. **Ory, S., H. Brazier, and A. Blangy.** 2007. Identification of a bipartite focal adhesion localization signal in RhoU/Wrch-1, a Rho family GTPase that regulates cell adhesions and migration. Biol. Cell **99:**701–716.
31. **Ozdamar, B., R. Bose, M. Barrios-Rodiles, H. R. Wang, Y. Zhang, and J. L. Wrana.** 2005. Regulation of the polarity protein Par6 by TGFbeta receptors controls epithelial cell plasticity. Science **307:**1603–1609.
32. **Pollack, A. L., R. B. Runyan, and K. E. Mostov.** 1998. Morphogenetic mechanisms of epithelial tubulogenesis: MDCK cell polarity is transiently rearranged without loss of cell-cell contact during scatter factor/hepatocyte growth factor-induced tubulogenesis. Dev. Biol. **204:**64–79.
33. **Qiu, R. G., A. Abo, and G. S. Martin.** 2000. A human homolog of the C. elegans polarity determinant Par-6 links Rac and Cdc42 to PKCzeta signaling and cell transformation. Curr. Biol. **10:**697–707.
34. **Rogers, K. K., T. S. Jou, W. Guo, and J. H. Lipschutz.** 2003. The Rho family of small GTPases is involved in epithelial cystogenesis and tubulogenesis. Kidney Int. **63:**1632–1644.
35. **Roh, M. H., S. Fan, C. J. Liu, and B. Margolis.** 2003. The Crumbs3-Pals1 complex participates in the establishment of polarity in mammalian epithelial cells. J. Cell Sci. **116:**2895–2906.
36. **Rojas, R., W. G. Ruiz, S. M. Leung, T. S. Jou, and G. Apodaca.** 2001. Cdc42-dependent modulation of tight junctions and membrane protein traf-

fic in polarized Madin-Darby canine kidney cells. Mol. Biol. Cell **12:**2257–2274.

37. **Ruusala, A., and P. Aspenstrom.** 2008. The atypical Rho GTPase Wrch1 collaborates with the nonreceptor tyrosine kinases Pyk2 and Src in regulating cytoskeletal dynamics. Mol. Cell. Biol. **28:**1802–1814.
38. **Sahai, E., and C. J. Marshall.** 2002. RHO-GTPases and cancer. Nat. Rev. Cancer **2:**133–142.
39. **Saras, J., P. Wollberg, and P. Aspenstrom.** 2004. Wrch1 is a GTPase-deficient Cdc42-like protein with unusual binding characteristics and cellular effects. Exp. Cell Res. **299:**356–369.
40. **Shen, L., and J. R. Turner.** 2005. Actin depolymerization disrupts tight junctions via caveolae-mediated endocytosis. Mol. Biol. Cell **16:**3919–3936.
41. **Shin, K., V. C. Fogg, and B. Margolis.** 2006. Tight junctions and cell polarity. Annu. Rev. Cell Dev. Biol. **22:**207–235.
42. **Shutes, A., A. C. Berzat, A. D. Cox, and C. J. Der.** 2004. Atypical mechanism of regulation of the Wrch-1 Rho family small GTPase. Curr. Biol. **14:**2052–2056.
43. **Stevenson, B. R., and D. A. Begg.** 1994. Concentration-dependent effects of cytochalasin D on tight junctions and actin filaments in MDCK epithelial cells. J. Cell Sci. **107:**367–375.
44. **Symons, M., and J. Settleman.** 2000. Rho family GTPases: more than simple switches. Trends Cell Biol. **10:**415–419.
45. **Tao, W., D. Pennica, L. Xu, R. F. Kalejta, and A. J. Levine.** 2001. Wrch-1, a novel member of the Rho gene family that is regulated by Wnt-1. Genes Dev. **15:**1796–1807.
46. **Vadlamudi, R. K., L. Adam, R. A. Wang, M. Mandal, D. Nguyen, A. Sahin, J. Chernoff, M. C. Hung, and R. Kumar.** 2000. Regulatable expression of p21-activated kinase-1 promotes anchorage-independent growth and abnormal organization of mitotic spindles in human epithelial breast cancer cells. J. Biol. Chem. **275:**36238–36244.
47. **Vadlamudi, R. K., and R. Kumar.** 2003. P21-activated kinases in human cancer. Cancer Metastasis Rev. **22:**385–393.
48. **Wolff, S. C., A. D. Qi, T. K. Harden, and R. A. Nicholas.** 2005. Polarized expression of human P2Y receptors in epithelial cells from kidney, lung, and colon. Am. J. Physiol. Cell Physiol. **288:**C624–C632.
49. **Yamanaka, T., Y. Horikoshi, A. Suzuki, Y. Sugiyama, K. Kitamura, R. Maniwa, Y. Nagai, A. Yamashita, T. Hirose, H. Ishikawa, and S. Ohno.** 2001. PAR-6 regulates aPKC activity in a novel way and mediates cell-cell contact-induced formation of the epithelial junctional complex. Genes Cells **6:**721–731.
50. **Zegers, M. M., L. E. O'Brien, W. Yu, A. Datta, and K. E. Mostov.** 2003. Epithelial polarity and tubulogenesis in vitro. Trends Cell Biol. **13:**169–176.